Asian Journal of Chemistry; Vol. 28, No. 10 (2016), 2325-2330

ASIAN JOURNAL OF CHEMISTRY

http://dx.doi.org/10.14233/ajchem.2016.19982

Microwave Assisted Preparation and Physico-Chemical Properties of Mixed Oxides Silica-Zirconia Montmorillonite K10 Nanocomposite

SERLY JOLANDA SEKEWAEL[1,*], KARNA WIJAYA[2], TRIYONO[2] and ARIEF BUDIMAN[3]

[1]Department of Chemistry, Faculty of Mathematics and Natural Sciences, Pattimura University, Ambon, Indonesia
[2]Department of Chemistry, Faculty of Mathematics and Natural Sciences, Gadjah Mada University, Yogyakarta, Indonesia
[3]Department of Chemical Engineering, Faculty of Engineering, Gadjah Mada University, Yogyakarta, Indonesia

*Corresponding author: Tel: +62 85243640076; E-mail: sjsekewael@yahoo.com

Received: 21 March 2016; *Accepted*: 25 May 2016; *Published online*: 30 June 2016; AJC-17990

A new solid material, silica-zirconia mixed oxides montmorillonite K10 nanocomposite was prepared through calcination process at various microwave radiation energy output and conventional method along with their characterization.The results show that microwave irradiation at 700 W enhanced the physico-chemical properties of montmorillonite K10. The increase of total surface acidity, specific surface area as well as the total pore volume, respectively. The slightly increased of basal spacing (d_{001}) caused the layers structure of mixed oxide silica-zirconia montmorillonite becoming more regular than untreated montmorillonite as investigated by TEM analyses.

Keywords: Montmorillonite K10, Mixed oxide silica-zirconia, Microwave radiation.

INTRODUCTION

Microwave assisted preparation of nanocomposite material is based on the efficient heating of materials by "microwave dielectric heating" effects. This phenomenon is dependent on the ability of a specific material to absorb microwave energy and convert it into heat. Two main mechanisms of heating *i.e.*, dipole polarization and ionic conduction caused by the electric component of an electromagnetic field. Hence microwave irradiation produces an efficient internal heating (in-core volumetric heating) by direct coupling of microwave energy with the molecules that are present in the reaction mixture [1]. One application of microwave energy for nanocomposite materials processing is calcination process. Calcination reaction was carried out using microwave radiation in order to decrease the consumption of two industrially important parameters *e.g.*, time and energy.

In this study, a new procedure for the synthesis of mixed-oxide silica-zirconia montmorillonite K10 nanocomposite was proposed. Montmorillonite K10 and structurally modified ion exchange (intercalation) or pillars, known to act as a catalyst Bronsted acid and Lewis acid for various organic reactions, as reported literally [2-5]. The synthesis is based on two specific characteristics of layer silicate montmorillonite clay. First, the silicate particles can be dispersed into individual layers, with a thickness of 1 nm. Secondly, the ability to improve the chemical properties of the surface with a cation exchange reaction. The negatively charged silica particles can be modified with zirconium polyoxocations, which then can easily be introduced between the silicate layers to form SiO_2–ZrO_2 nanocomposite clays. For this purpose, colloidal particles of mixed oxide SiO_2–ZrO_2 were prepared *via* a sol-gel process [6,7]. Positively charged metal oxide sols may be intercalated into the interlayer of montmorillonite by cation-exchange reactions, providing nanocomposite materials after calcinations [8].

The physico-chemical properties of host montmorillonite and mixed oxide silica-zirconia montmorillonite K10 nanocomposite were systematically investigated by X-ray diffraction, nitrogen adsorption isotherm measurement, X-ray fluorosence, Fourier transform infrared spectrophotometry, transmission electron microscopy as well as scanning electron microscopy methods. Total surface acidity was determined by ammonium-gravimetric method.

EXPERIMENTAL

All the chemicals were commercially available and were used without further purification. Montmorillonite K10 (hereafter Mt-K10) was obtained from Fluka (Chemica), TEOS, $ZrOCl_2 \cdot 8H_2O$, HCl, ethanol, NaOH, distilled water, akuabides, ammonia and Whatman filter paper were used as received.

General preparation of mixed oxides silica-zirconia pillared montmorillonite K10: Mixed oxide silica-zirconia Mt-K10 nanocomposite were synthesized by sol gel process and intercalation followed by calcination. By using Han and

Yamanaka [7] method, we prepared sol silica by mixing 41.6 g TEOS, 10 mL HCl 2 M and 12 mL ethanol at room temperature for 2 h. Solution was then mixed with 0.2 mol/L $ZrOCl_2 \cdot 8H_2O$ with molar ratio of [Si]/[Zr]=10/1. The mixture was titrated with a 0.2 mol/L NaOH solution until the pH maintained at about 1.5. The dispersion was allowed to stand for 1 h at room temperature and then mixed with Mt-K10 dispersion 1 % w/v at a molar ratio Si/Zr/CEC = 50/5/1. Cation exchange capacity (CEC) of Mt-K10 is 43.6 me/100 g. The mixture was allowed to stand for 20 h under stirring at room temperature. Centrifugation was used to separate the product followed by washed with ethanol/water (1:1 volume ratio) and then dried at room temperature. The dried samples were subjected to microwave radiation energy output 700 W and 800 W for 10 min, respectively. The products were mixed oxide silica-zirconia montmorillonite K10 nanocomposites, encoded as SZMK-700 and SZMK-800. For comparison purpose, the dried samples before calcination and conventional calcination for 2 h at 400 °C were prepared, encoded as SZMK-SK and SZMK-KB.

Characterization: All samples were analyzed by X-ray diffraction, XRD-6000 Shimadzu, using CuK_α powder irradiated by λ = 1.5406 Å. Operating conditions: acceleration voltage 40 kV, current 30 mA, slit width of 0.05 and a scanning speed of 5 °/min. X-ray diffraction patterns of the samples were recorded from 2θ between 2-40° and came out as a diffractogram of data to be further analyzed to determine changes in the basic range d_{001}.

N_2 adsorption-desorption isotherms were measured at liquid nitrogen temperature with a gas sorption analyzer (Quantachrome, NOVA 11000). Prior to measurement, samples were degassed at 300 °C for 3 h under reduced atmosphere. Furthermore, all samples were cooled with liquid nitrogen to form a single layer of nitrogen molecules on the surface of the samples. Adsorption-desorption isotherms for nitrogen were recorded on the system 1-MP automated gas at liquid nitrogen temperature of 77.4 K. With a measured change in pressure and volume or weight of gas adsorbed by the sample accordingly the specific surface area, pore volume, pore size distribution and adsorption isotherm can be determined.

FTIR spectra were obtained from KBr (analytical grade and dried at 110 °C) pressed disks of about 12 mm diameter and 1 mm thickness prepared by applying about 8×10^3 bar pressure for 10 min on finely ground particles containing about 3 mg of material and 97 mg of KBr in the range 4000-400 cm^{-1} using Shimadzu PC8201 infrared spectrophotometer.

Characterization by TEM using TEM JEOL-1400. Samples were prepared in advance through the fixation process of making an incision and coating to obtain a very thin specimen. The specimen placed on a TEM grid was then shot by the electron beam energy with very high (accelerated at a voltage of 120 keV). Sample images in the form of micrographs were analyzed.

SEM images were recorded on a SEM JEOL JSM-6510. Sample was first coated with gold metal, then placed in a holder which is covered with a layer of carbon and then analyzed by SEM using SE detector (secondary electron), which operated under the conditions: acceleration voltage of 20.0 kV; probe current 1.00000 nA; counting rate 3337 cps.

Sample and standard Zr enumerated by XRF instrument, XRF-EG & GORTEG7001. Spectra which appear in the energy range 0-50 keV were analyzed with reference to a standard Zr to determine the concentration of Zr in the sample.

Total surface acidity of solids was conducted by ammonium adsorption followed by FTIR measurements. The sample was placed in a desiccator and evacuated by a vacuum pump for 1 h before ammonium vapour exposing for 24 h. The sample was then evacuated for 1 h at the room temperature and then analyzed by a PC8201 infrared spectrophotometer. Total acidity of the samples were measured using graphimetric method.

RESULTS AND DISCUSSION

Fig. 1 shows a series of XRD patterns of Mt-K10, SZMK-SK, SZMK-KB, SZMK-700 and SZMK-800. Mt-K10 shows diffraction peaks at 8.79° (001), 17.71° (003), 19.72° (100), 26.56° (005) and 34.89° (105) corresponding to montmorillonite of hexagonal phase. These diffraction peaks are similar to that reported [9,10]. Ghebaur *et al.* [9] reported the (001) reflection at 2θ = 8.90° (d = 0.98 nm) for Mt-K10. In this case, Mt-K10 showed (001) reflection at 8.79° (d = 1.005 nm) while SZMK-SK (sample before calcination) slightly shifted to lower angle 8.38° (d = 1.054 nm) depicting the slight increase of interlayer distance. Intercalation process make the basal spacing increase [6,11]. Upon calcination at 700 W, SiO_2-ZrO_2 nanosol transform into mixed oxides with a basal spacing of 1.013 nm and the peak virtually unchanged compared to the Mt-K10, which is showing weak changes of crystallinity. This is indicated sufficient retention of crystallinity during the preparation procedure.

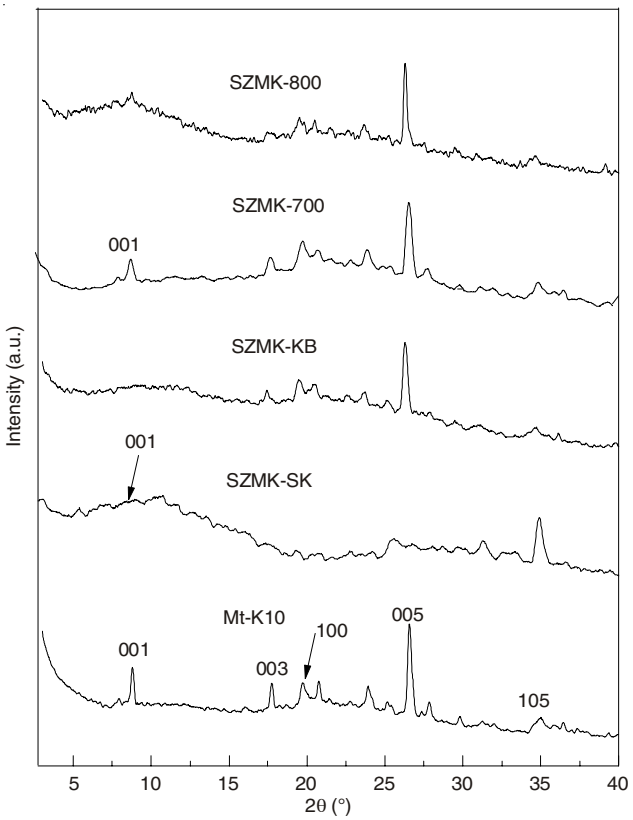

Fig. 1. Diffractogram of Mt-K10, SZMK-SK, SZMK-KB, SZMK-700 and SZMK-800

A basal reflection of montmorillonite does not appear on the conventionally calcined sample (SZMK-KB) as well as sample that treatment using microwave radiation 800 W. This is clear from three main peaks of difractogram. It may be due to the effect of heating. Contraction of the pillars and dehydroxylation of silicate affects the basal spacing gradually decrease on heating [7]. We can say that the calcination with microwave radiation 700 W produce a better structure than 800 W and conventional calcination.

The XRD data show that there is no significant increase in the interlayer distance indicating that silica-zirconia nanoparticles are not intercalated well within the lamellar structure, otherwise it found to deposited on the external surface of Mt-K10 in SZMKs [10]. According to Choy *et al*. [6], when the colloidal particles have been entered the layers of montmorillonite then the Δd_{001} value of interlayer space become 1.24 nm, by subtracting the thickness of the silicate layer (0.96 nm).This value is much greater from our results. It might be due to the host material we used was acid-activated montmorillonite which have undergone dealumination and the possibility of having a smaller layer thickness than the thick layer of montmorillonite itself, also the increase in interlayer distance has not been sufficient enough to house silica-zirconia nanoparticles within their layers. This is supported by morphological data. The results of the nitrogen adsorption analysis of the samples were presented in Table-1.

TABLE-1
NITROGEN GAS ADSOPTION ANALYSIS

Sample	Specific surface area ($m^2 g^{-1}$)*	Total pore volume ($cm^{-3} g^{-1}$)**	Average pore radius (Å)
Mt-K10	240	2.43	32.92
SZMK-KB	134	1.17	35.94
SZMK-700	249	2.69	29.32
SZMK-800	170	1.71	57.54

*Determined by the multipoint BET method.
**Determined using BJH pore analysis.

SZMK-700 have a higher specific surface area compared to Mt-K10, SZMK-800 and SZMK-KB. This is associated with small average pore radius and large total pore volume from the entire surface of the pores themselves. Theoretically, the pillarization enhances specific surface area parameter regarding the formation of the metal oxide pillar between interlayer space of a montmorillonite structure [12]. Slightly increased in specific surface area of SZMK-700 compared to Mt-K10 indicating that the colloidal particles are more aggregates on the pore surface of SZMK-700 nanocomposite itself than its function as a pillar, as proved by SEM images. Our experiment on all samples suggests the consistence in the high total pore volume gives the high specific surface area, but inconsistence in average pore radius for SZMK-800 and SZMK-KB. Furthermore, the N_2 adsorption data showed that the calcinated samples assisted by microwave radiation have a higher specific surface area compared to the conventional one. It is also shown that specific surface area and total pore volume decreased with the increasing of microwave radiation power.

The nitrogen adsorption-desorption isotherm of Mt-K10 and SZMKs are presented in Fig. 2. The isotherms of all samples were similar and almost had the same shape. They corresponded to type IV according to BDDT classification [13], where most of the nitrogen is adsorbed in mesopores of the nanocomposite materials and their hysteresis loops are of type H3 according to the IUPAC classification, indicating the presence of slit-shape pore [6,14]. Adsorption of non-polar gases by montmorillonite clays and the aggregates of other platy particles typically given the type H3 of the hysteresis loop, as reported [15,16]. Our experiment clearly demonstrated that the nitrogen uptake increase continuously. This is exist because the pores are not so narrow that they can accommodate more than a single molecular layer on their walls. The presence of mesoporous brings about an increase in adsorption.

Both samples, SZMK-700 and SZMK-800, prepared with the microwave radiation adsorbed more nitrogen than conventional calcinated sample SZMK-KB. These results are consistent with the data specific surface area (Table-1). The function of microwave radiation in the calcination of montmorillonite offers advantages over conventional methods, including a higher heating rate in a shorter time, due to volumetric heating [17]. Compared to conventional heating methods, the microwave technique also provides uniform heating. Larger specific surface area of the adsorbent adsorbs more gas volume. Furthermore, this was proved by the slope of the graph sharper in the P/P_0 0.4-0.5 for adsorption and desorption isotherms branch of SZMK-800 and SZMK-700. Instead, SZMK-KB has a more gentle slope graph.

Fig. 3 shows the pattern of the pore size distribution of all samples calculated by BJH method. This figure shows a wide pore size distribution of all samples, which has a microporosity with a narrow size distribution and exhibits a population of mesopores. The pore size distributions of SZMKs samples (Fig. 3) are slightly different to that described for Mt-K10. It might be due to an increasing in the proportion of macropores when Si-Zr is added to the system.

Fig. 4 shows the FTIR spectra of host montmorilonit, Mt-K10 and silica-zirconia Mt-K10 nanocomposites. Absorption region is divided into two groups, functional group region between 4000 to 3000 cm^{-1} and finger print region between 1400 to 400 cm^{-1}. There were several important absorption bands for identification of Mt-K10 and silica-zirconia Mt-K10 nanocomposite, such as bands at 3749, 3441, 2368, 1635, 1056, 794 and 462 cm^{-1}. Those bands are similar to those reported in literature for Mt-K10 [18].

The absorption band at 3749 cm^{-1} is identified as -OH stretching vibration of structural octahedral Al-OH. Strong broad bands in 3441 cm^{-1} region are due to structural -OH stretching vibration of water molecules. This band is reinforced with bending vibration bands at 1635 cm^{-1}. This is an indication that montmorillonite has a water absorbing properties. Stretching vibration of water molecules became weak and have medium intensity for the SZMKs nanocomposite, except for SZMK-SK (sample before calcination). Molu and Yurdakoç [18] reported that pillaring process replaces a large amount of hydrated interlayer cations and it decreased absorption band intensity. A decrease of OH absorption on SZMKs nano composites is due to dehydration and dehydroxsylation experienced during thermal agitation when the microwave

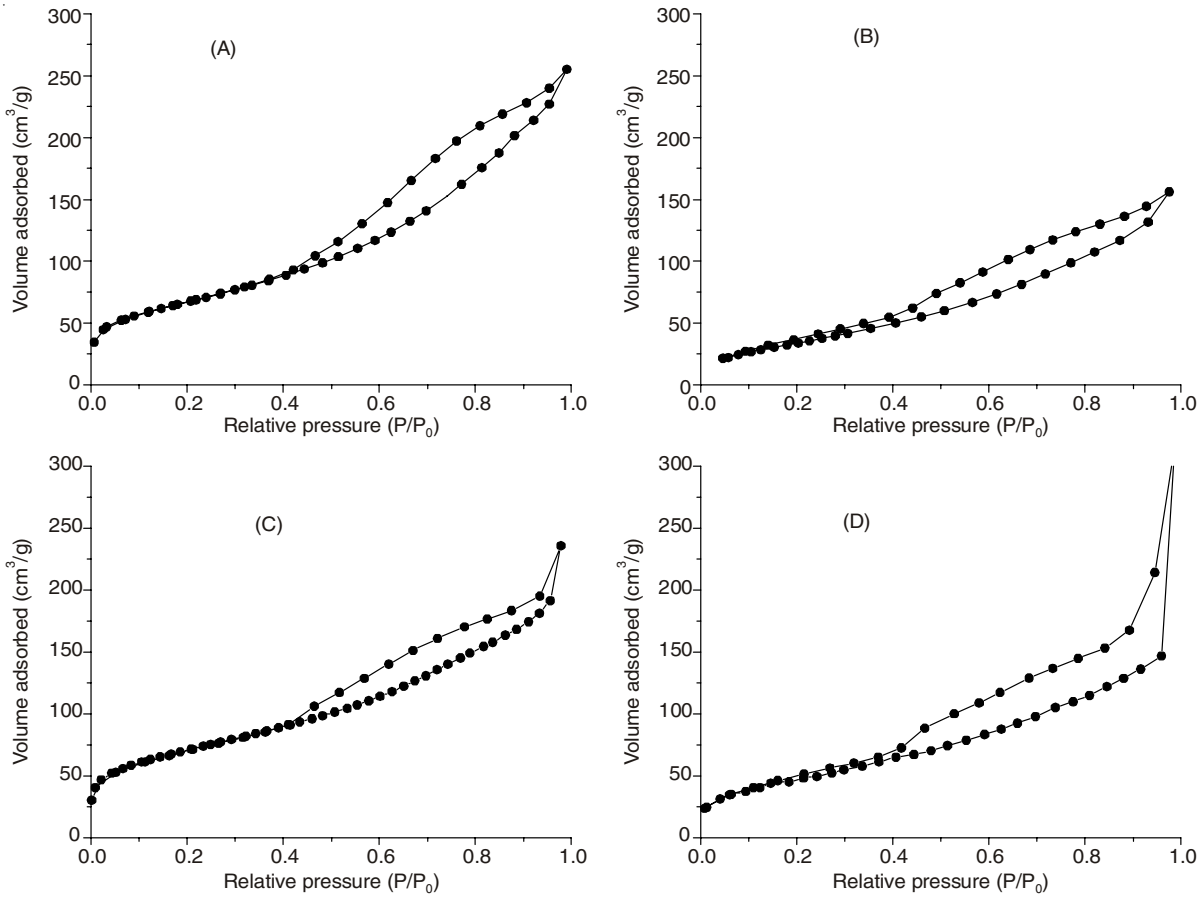

Fig. 2. Nitrogen adsorption-desorption isotherms of (A) Mt-K10, (B) SZMK-KB, (C) SZMK-700, (D) SZMK-800

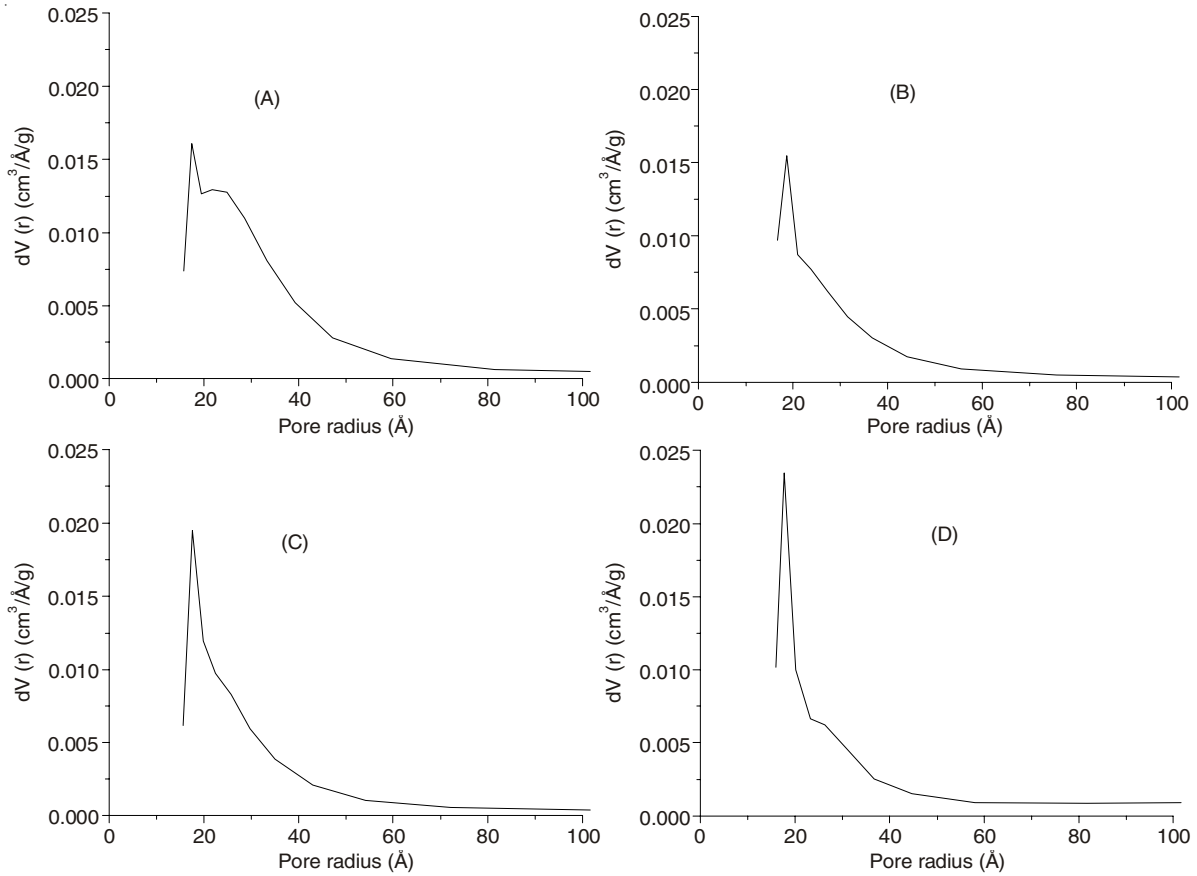

Fig. 3. Pore size distribution data of (A) Mt-K0, (B)SZMK-KB, (C) SZMK-700, (D) SZMK-800

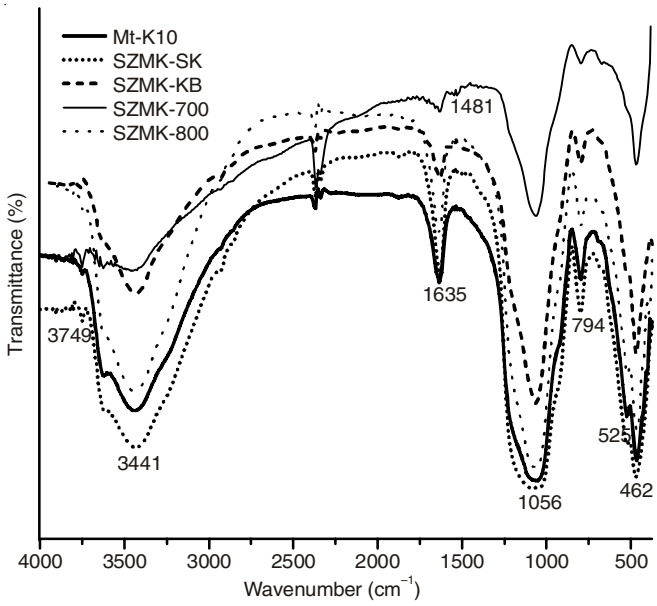

Fig. 4. FTIR Spectra of Mt-K10, SZMK-SK, SZMK-KB, SZMK-700 and SZMK-800

radiation and the conventional calcination process takes place. Two bands at around 1056 and 462 cm^{-1} are characteristic of asymetric stretching and bending vibrations of SiO_2 (Si-O-Si) in the tetrahedral layer as reported in silicate system [19]. The bands are slightly shifted to larger wavenumbers and the absorption intensity becomes narrow due to increase of Si/Al ratio.

The band at 794 cm^{-1} is due to stretching vibration of Al_{IV} tetrahedra. The absorption band at 525 cm^{-1} corresponding to the bending vibration of Al-Si-O is disappearing almost completely after calcination process, indicating the dealumination of silicate layer.

Absorption in the fingerprint region is still observed in the SZMKs nanocomposites, indicating that the thermal conversion process does not damage the bond of Si-O or Al-O in silicate interlayers of montmorillonite. This means that the basic structure of the montmorillonite layer is not affected by the pillaring process [18]. The weak band at 1481 cm^{-1} of SZMK-700 is might be due to the vibration of OH groups of the intercalated zirconium species which decreases after heating at 800 W or even at 400 °C and it is assigned as Lewis acid sites [7,12]. It is also proved that mixed oxides SiO_2/ZrO_2 contributed the acidity of the nanocomposite.

After some initial characterization in this work, it is concluded that the power input 700 W of microwave radiation enhanced physico-chemical properties of the nanocomposite material. Furthermore, the nanocomposite SZMK-700 was characterized using XRF, TEM as well SEM. The total surface acidity to support the data was also calculated.

TEM micrograph presented in Fig. 5 shows the morphology of multilayer silicate montmorillonite of Mt-K10 and SZMK-700. The Mt-K10 interlayer space estimated from the TEM image was around 1.005 nm, which is similar to that calculated from the (001) reflection on XRD data, while the SZMK-700 interlayer space was 1.017 nm, slightly higher than 1.013 nm calculated from the (001) reflection on XRD data. The silicate layer of SZMK-700 is more regular after the pillarization by a mixture of metal oxides SiO_2-ZrO_2 using microwave irradiation. This indicates that the two phases of the mixed oxide and the silicate layers Mt-10 bound well. This means that the SiO_2-ZrO_2 mixed oxides permanently connecting montmorillonite sheet silicate. Microwave heating is expected to lead to a narrow size self-assembled distribution of nanoparticles [1]. The intercalated nanocomposite is obtained if atleast one polymer chains intercalated between silicate layers produces multilayer morphology is well ordered and constructed of intercalated organic and inorganic layers [20].

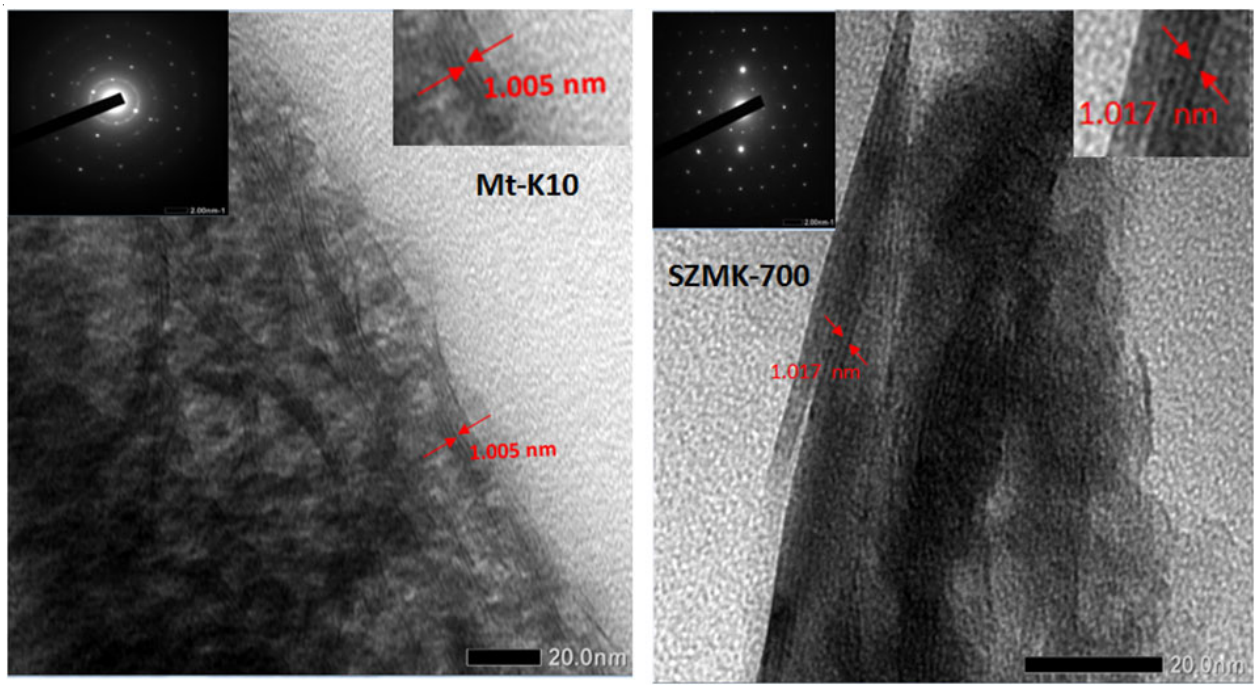

Fig. 5. TEM images and SAED patterns (insert) of Mt-K10 and SZMK-700

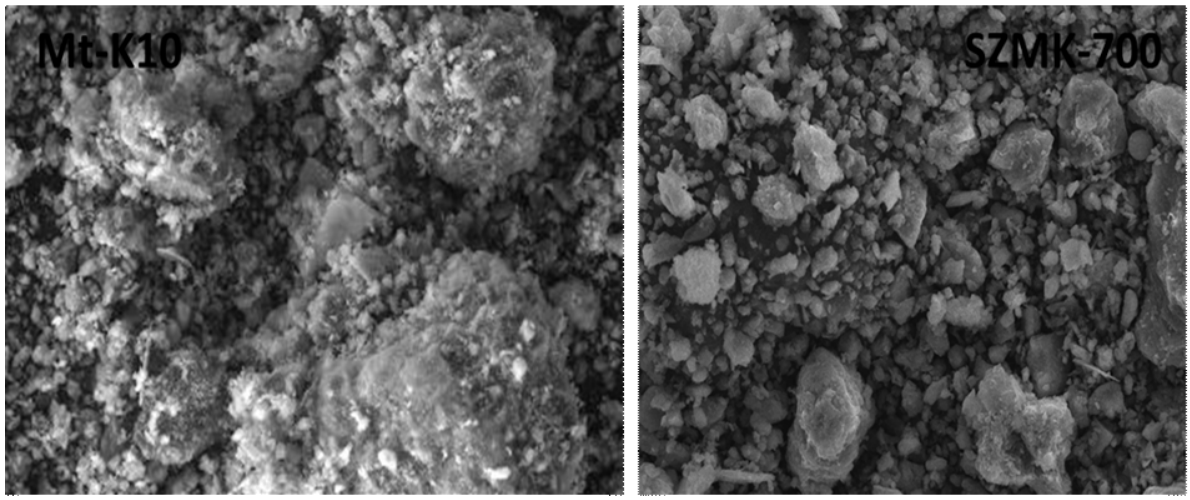

Fig. 6. SEM images of Mt-K10 and SZMK-700

The electron diffraction patterns corresponding to TEM images displayed several spots, which were tended to change into rings during the observation. Because each spot in accordance with the conditions of the crystal structure diffraction of the samples, it can be concluded that the electron diffraction patterns of the Mt-10 and SZMK-700 describe the crystal structure of the two samples are similar and there is almost no crystal defects. This is consistent with the XRD data where the crystallinity of the samples is almost unchanged.

Fig. 6 shows the SEM images of interlayer structure Mt-K10 and microwave radiated sample, SZMK-700, with 500x magnification. SEM was used to probe the change in morphological features after calcination process. Both samples show the typical structure of porous material and surface morphology exhibited rough and disordered structure. A similar behaviour reported by Muthuvel *et al*. [21] for Fe encapsulated montmorillonite K10. The pillaring process made the particle morphology of the sample changes slightly and a different agglomeration state can be inferred from these observations. SZMK-700 has more pores between particles than Mt-K10. Also, SZMK-700 appears to be highly compact, so it is seen that the inter-particle pores are smaller in the SZMK-700 sample, compared to the Mt-K10.

XRF calculations show the Zr content of Mt-K10 and SZMK-700 nanocomposites were equal to 0 and 2.6418 %, respectively. It may be confirmed that Zr species coating the surface of SiO_2 sol nano-sized particles and exist in the interlayer of montmorillonite [6]. Effect of Si-Zr oxides in prepared materials on the total surface acidity were measured by ammonia-adsorption, calculated using the gravimetric method. Total surface acidity measurement was 4.83 and 4.99 mmol/g for Mt-K10 and SZMK-700, respectively. In this case, prepared materials SZMK-700 assisted by microwave radiation exhibited a more total surface acidity.

Conclusion

Present research proves that the mixed oxide silica-zirconia montmorillonite nanocomposite can be prepared by above stated methods and the calcination with the microwave radiation assited is proven to improve the physico-chemical properties of the nanocomposite materials.

ACKNOWLEDGEMENTS

The authors thank to Kemenristek Indonesia in cooperation with the University of Gadjah Mada in INSINAS Project 2014, which has funded for this publication.

REFERENCES

1. U. Riaz and S.M. Ashraf, *Appl. Clay Sci.*, **52**, 179 (2011).
2. R.D. Aher, M.H. Gade, R.S. Reddy and A. Sudalai, *Indian J. Chem.*, **51A**, 1325 (2012).
3. M. Ayoub and A.Z. Abdullah, *Catal. Commun.*, **34**, 22 (2013).
4. R. Fazaeli and H. Aliyan, *Appl. Catal. A*, **331**, 78 (2007).
5. M.M. Hashemi, B. Eftekhari-Sis, A. Abdollahifar and B. Khalili, *Tetrahedron*, **62**, 672 (2006).
6. J.H. Choy, J.B. Yoon, H. Jung and J.H. Park, *J. Mater. Chem.*, **13**, 557 (2003).
7. Y.S. Han and S. Yamanaka, *J. Solid State Chem.*, **179**, 1146 (2006).
8. Ruslan, K. Wijaya and Triyono, *Int. J. Appl. Chem.*, **9**, 15 (2013).
9. A. Ghebaur, S.A. Garea and H. Iovu, *U.P.B. Sci. Bull. Series B*, **73**, 169 (2011).
10. J.P. Kumar, P.V.R.K. Ramacharyulu, G.K. Prasad and B. Singh, *Appl. Clay Sci.*, **116-117**, 263 (2015).
11. A. Suseno, K. Wijaya, W. Trisunaryanti and M. Shidiq, *Asian J. Chem.*, **27**, 2619 (2015).
12. A. Gil, S.A. Korili, R. Trujilano and M.A. Vincente, Pillared Clays and Related Catalyst, Springer Science+Business Media, New York (2010).
13. S.J. Gregg and K.S.W. Sing, Adsorption, Surface Area and Porosity, Academic Press, London (1982).
14. P. Yuan, F. Annabi-Bergaya, Q. Tao, M. Fan, Z. Liu, J. Zhu, H. He and T. Chen, *J. Colloid Interf. Sci.*, **324**, 142 (2008).
15. R.M. Barrer, *Pure Appl. Chem.*, **61**, 1903 (1989).
16. K.S.W. Sing and R.T. Williams, *Adsorpt. Sci. Technol.,* **22**, 773 (2005).
17. S. Korichi, A. Elias, A. Mefti and A. Bensmaili, *Appl. Clay Sci.*, **59–60**, 76 (2012).
18. Z.B. Molu and K. Yurdakoç, *Micropor. Mesopor. Mater.*, **127**, 50 (2010).
19. H. Van Olphen and J.J. Fripiat, Data Handbook for Clay Minerals and Other Non-metallic Minerals, Pergamon Press, Oxford, England (1979).
20. M. Alexandre and P. Dubois, *Mater. Sci. Eng.*, **28**, 1 (2000).
21. I. Muthuvel, B. Krishnakumar and M. Swaminathan, *Indian J. Chem.*, **51A**, 800 (2012).